2012

Phase Estimation with Two-Mode Squeezed Vacuum and Parity Detection: Bayesian Analysis

Keith Motes

Phase Estimation with Two-Mode Squeezed Vacuum and Parity Detection: Bayesian Analysis

Keith R. Motes,[1,*] Petr M. Anisimov,[1] and Jonathan P. Dowling[1]

[1] *Hearne Institute for Theoretical Physics and Department of Physics and Astronomy Louisiana State University, Baton Rouge, LA 70803*

[*] *Corresponding author: kmotes1@lsu.edu or motesk@gmail.com*

This paper is designed to fulfill my honors thesis requirement for graduating with upper division honors at LSU. For this project I am expanding upon my research titled, "Phase estimation with two-mode squeezed vacuum and parity detection: Bayesian analysis."

The first half of this thesis expands upon the background of my research work by discussing the quantum interferometer and the states of light traveling through it in detail. I explain why phase estimation is important, the fundamentals of quantum optics, review classical interferometry, and describe quantum interferometry by considering two specific quantum states that can be used. I will also show how quantum mechanics is used to improve phase sensitivities by twelve or more orders of magnitude.

The second half of this paper discusses a recently proposed phase-estimation protocol that is based on measuring the parity of a two-mode squeezed vacuum state at the output of a Mach-Zehnder interferometer which shows that sub-Heisenberg sensitivity can be obtained [P. M. Anisimov, et al., Phys. Rev. Lett. **104**, 103602 (2010)]. This sensitivity, however, is expected in the case of infinite number of parity measurements. Here we consider a case of finite number of parity measurements implemented with photon-number-resolving detectors and we use Bayesian analysis to characterize the sensitivity of the phase estimation in such a scheme. We have found that phase estimation becomes biased near 0 or $\pi/2$ phase values. Yet there is an in-between region where the bias becomes negligible. In this region, our phase estimation scheme saturates the Cramer-Rao bound and beats the shot noise limit.

1. Introduction

Phase estimation is the primary tool for optical metrology. A cheap and practical way to estimate phase is to use an interferometer. An interferometer is an instrument that uses wave interference to make precise measurements of phase difference in terms of wavelength. The first interferometer was invented my Albert Michelson in 1891 as a means to successfully determine the speed of light [1]. The idea of using an interferometer to make measurements has been used for many things since the famous Michelson-Morley experiment such as attempting to detect gravitational waves. The downside to this standard interferometer is that the precision of its measurements are very limited compared to the accuracy needed in so many modern day experiments and technologies because it is being used classically [2]. Thus, one needs to improve upon these classical interferometers if we are to ever do things such as travel to distant solar systems, give us Star Wars like technology like light sabers, and harness the power of quantum computing.

Luckily, quantum mechanics offers the tools necessary to improve upon the phase measurements in an interferometer. Its sensitivity improves by inputting quantum states of light into the interferometer instead of classical ones. The field of quantum optics describes these quantum states of light. Quantum optics is the study of light using the wave-particle duality of photons. By combining measurements of the statistical wave nature of photons with the fact that they can be observed discretely grants one the ability to improve upon the way things are done classically [3]. In 1977, Kimble demonstrated the first source of light requiring a quantum mechanical description. This was a single atom that emitted one photon at a time [4]. This quickly led physicists to develop the laser which has a myriad of applications. The quantum mechanical description of the laser is given by what is called a coherent state of light [5]. One important property of the coherent state is that the light is polarized. This means that individual photon in the laser vibrates in the same direction. This is quite amazing seeing as there are billions of photons in even a small laser beam. As I will show in the section titled coherent state, this discovery led to around twelve orders of magnitude of improvement in the sensitivity of phase estimation in a Mach-Zehnder interferometer (MZI). Since then many others have been discovered expanding interest among researchers in hot topics such as gravitational wave detection, attosecond light pulses for improving the precision of atomic clocks, Bose-Einstein condensates, and particularly quantum information technology [6].

Since the discovery of the coherent state there has been many other quantum states of light devised based on principles from quantum mechanics such as entanglement and spin-orbit coupling. One such class of states is called squeezed states [7]. These squeezed quantum states of light offers much to quantum optics by allowing for more accurate measurements as demanded by modern day research and development.

My research uses a recently proposed phase-estimation protocol that is based on measuring a signal at the output of a quantum interferometer that comes from a certain squeezed state of light. There are several experimental ways to do this but coherent light based interferometry is most commonly used. The downside to coherent states is that its sensitivity for phase estimation is limited by the shot-noise. This is not a problem in the case of limitless resources or in the case of samples that can withstand large doses of radiation; however, this is a problem otherwise, and one has to resort to interferometry with quantum states of light, such as N00N states [8], that demonstrate sub-shot-noise or even Heisenberg limited (HL) sensitivity of phase estimation.

2. Classical Interferometry

2.A. What is a Classical Interferometer?

A classical interferometer is an instrument that uses wave interference to make precise measurements of phase difference in terms of wavelength. It is considered classical because it uses a constant beam of light or other electromagnetic wave produced by an instrument such as a laser where a simple 'classical' intensity measurement can be made. Fig. 1a shows a Michelson interferometer (MI), which is the most common configuration for optical interferometry and was invented by Albert Abraham Michelson. It is the most common type of classical interferometer used by experimentalists and was first used in what is called the Michelson-Morley experiment which provided evidence for special relativity [1]. Fig. 1b shows a Mach-Zehnder interferometer (MZI) which is mathematically equivalent to the MI but is used more by theorists because it is easier to visualize what happens in various parts of the interferometer. These interferometers both consist of several key components. These include an instrument that inputs some state of light, beam splitters (BS) that reflect and transmit light, mirrors that simply reflect light, a phase shifter that changes the state of light used, detectors to make measurements on the states at the output, and an analyzer such as a computer to interpret data and find the phase shift ϕ. The paths from the input instrument to the detectors are called the arms of the interferometer. My research is based on the part that comes after detection, which is to come up with an algorithm to program the analyzer with and accurately determine the phase shift ϕ.

In most commonly used interferometric setups and for the purpose of this paper one uses 50:50 beam splitters. This means that half of the intensity of the state of light used is transmitted while the other half is reflected. Upon every reflection of our beam there is a $\pi/2$ shift in the phase of the light. The phase shifter depends on what it is we are trying to measure. Some examples of what can cause a phase shift is when the light travels through a different medium or when the length of the arms of the interferometer change. The latter is the case of LIGO which attempts to measure gravitational waves predicted by

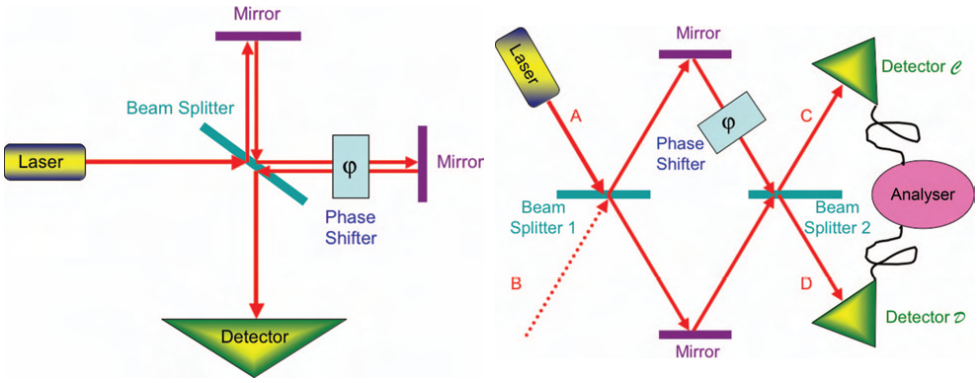

(a) Michelson Interferometer (b) Mach-Zehnder Interferometer

Fig. 1: (a) The Michelson interferometer which is commonly used in experimental optics and is essential for optical metrology. (b) The Mach-Zehnder interferometer often used by theorists to simplify the conceptual happenings in the MI.

Einstein's general theory of relativity. What causes the path length difference in the arm are gravitational waves from distant objects such as exploding super nova. When a gravity wave passes by LIGO it will change the length of the arms of the interferometer causing a phase shift that we want to measure. If the arms were parallel then the wave would change the lengths of the arms at LIGO by the same amount causing a zero net change in the difference between the lengths of the two arms, which means that we cannot detect a phase shift and thus can't detect the gravitational wave. As one can see from the overhead view of LIGO in Fig. 2, the arms of LIGO are perpendicular. In general we would expect a wave to only significantly change the length of one of the arms by some amount instead of both of them allowing us to determine some overall phase shift.

2.B. How Can We Make a Measurement?

Let's consider one steady laser beam being sent into port A as shown in the MZI of Fig. 1b. Since light is only inputted in port A and none in port B we call this 'one-mode.' When the beam hits BS 1 half of the intensity is transmitted and half is reflected. The different paths may be of different lengths or be composed of different materials to create this phase shift [1]. The beam hits the second 50:50 beam splitter where finally detectors C and D will measure some intensity. Let's define the intensity measured at each port and their difference M to be as follows:

$$I_C = I_A Sin^2(\phi/2), \tag{1}$$

$$I_D = I_A Cos^2(\phi/2), \tag{2}$$

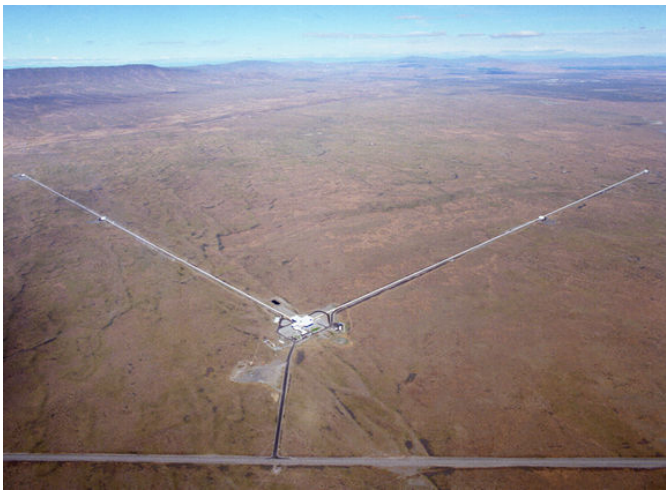

Fig. 2: This figure shows an overhead view of the Laser Interferometer Gravitational-Wave Observatory (LIGO). The perpendicularity of the arms at LIGO allow for the path length to only be changed in one arm when a gravity wave passes by.

$$M = I_D - I_C = I_A Cos(\phi/2) \tag{3}$$

Let's first consider the scenario where no phase shifter is present and remember the fact that there is a $\pi/2$ phase shift upon every reflection. Now trace out the path where the light reflects off of BS 1 and BS 2 and ends up in detector C. There are a total of three reflections which puts this beam at a phase of $3\pi/2$. Next, trace out the path where light is transmitted through both BS 1 and BS 2 and ends up in detector C. This path has one reflection which corresponds to this beam being $\pi/2$ out of phase. Since these two beams are exactly π out of phase with each other, they will exactly cancel and we will end up with a measurement of zero intensity in detector C. Now trace the two possible paths to detector D and one will find that both beams obtain a π phase shift and are thus exactly in phase with each other. This means that we would expect to see all of the intensity in detector D if no phase shifter is present.

In reality there is a phase shifter present or else there is little reason to perform such an experiment in the first place. We can determine this phase difference by using Eq. 3 because we already know the input intensity I_A and the difference intensity M can be measured by measuring the intensities I_C and I_D at port C and D respectively. Once we have the difference intensity M we can find the phase shift ϕ since we know I_A. The distance that our two beams are out of phase with each other, which we shall call x, can then be calculated by solving the simple relations $\phi = kx$ and $k = 2\pi/\lambda$. k is the wave number and λ is the wavelength of the beam inputted into port A [2].

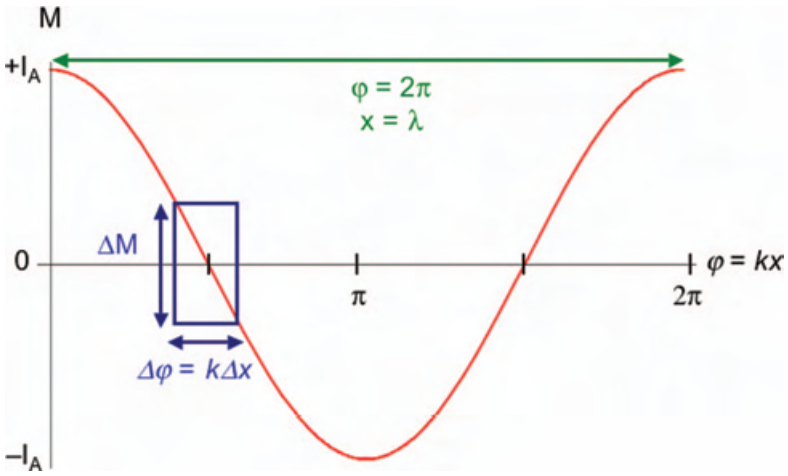

Fig. 3: The difference intensity M versus the phase difference ϕ is shown for the classical state. The slope of this line allows one to determine the best possible phase sensitivity for a given state of light.

2.C. How Sensitive can Classical Interferometry be?

One can analyze the sensitivity of this classical interferometer by looking at a plot of the difference intensity M versus the phase difference ϕ as shown in Fig. 3.

The blue box in Fig. 3 represents the uncertainty of our measurement where ΔM is the optical intensity fluctuation, $\Delta\phi$ is the phase shift fluctuation, and Δx is the minimum detectable displacement. If these quantities are small then we can approximate the slope using differentials by $\Delta M/\Delta\phi \approx \partial M/\partial\phi = I_A Sin\phi$. By solving this relation for $\Delta\phi$ we obtain the following equation:

$$\Delta\phi = \frac{\Delta M}{I_A Sin\phi} \tag{4}$$

After plugging in $\Delta\phi = k\Delta x$ and $k = 2\pi/\lambda$ into Eq. 4 we find that $\Delta x \propto \lambda$. It seems that the best sensitivity that one can achieve is on the order of the wavelength that is put into port A of the MZI. A typical laser has a wavelength on the order of a micron which limits our sensitivity to about $10^{-6}m$. While measurements of this order have many useful applications, one runs into a major problem when trying to measure something as sensitive as a gravitational wave at LIGO. These waves are predicted to only cause a path length difference of about $10^{-18}m$ at largest. Falling twelve orders of magnitude too short we need a method for improving this sensitivity. In the following I explain a method to do this using quantum interferometry.

3. Quantum Interferometry

Quantum interferometry considers the fluctuations of light intensity due to the probabilistic nature of the photon and harnesses its unique quantum effects to perform measurements on the phase which can be many orders of magnitude more sensitive than what can be done classically. The classical interferometer simply measures with intensities averaged over all of the photons. In this section I will consider the coherent state of light and a squeezed state of light. I will then start the second half of my thesis which describes how I use a specific squeezed state of light called Two-mode Squeezed Vacuum (TMSV) to design an analyzer than can accurately and cheaply determine the unknown phase shift that is so crucial to the advancement of many technologies.

3.A. Coherent State

Light can be described as both an electromagnetic wave and as a continuous stream of photons. Photons travel at the speed of light c with energy $E_\gamma = hf$ and are described by a quantum mechanical wave function spread over space. The coherent state of light is one way to describe light so as to make measurements on its energy and photon number. It was introduced by George Sudarshan in 1963 [9]. The dynamics of a coherent state closely resembles that of the classical harmonic oscillator [10] in that the energy of each photon can be described and measured individually. One important application of this state is that it approximately describes the output of a laser at a given frequency. Poissonian photon number statistics can be used with this state by summing over the energy of each individual photon. This allows better sensitivities to be achieved over their classical counterparts [5]. For the purposes of this paper the coherent state is generated by a laser and is denoted as $|\alpha\rangle$.

A coherent state fluctuates evenly in its intensity and phase, so we can estimate the phase as well as know the position of a photon at a given intensity. The way to describe the effects that the environment has on these photons and thus describe the phase shift ϕ is by the use of field operators. Specifically, the creation and annihilation operators are used to describe the addition or removal of photons from our system [11]. These field operators are essential to determining how the phase shifter changes our quantum states in an interferometer.

The coherent state is mathematically defined to be the right eigenstate of the non-hermitian annihilation operator $\hat{\alpha}$ [5]. A Hermitian operator is an operator that satisfies $A = A^\dagger$. We know that the eigenvalues of a Hermitian operator are real and that all eigenvectors corresponding to distinct eigenvalues are orthonormal. Since our annihilation operator $\hat{\alpha}$ is non-Hermitian, we may obtain eigenvalues that are imaginary and eigenvectors that are not orthonormal. As usual, if we would like to change a quantum state $|\mathbf{\Psi}(\mathbf{r}, t)\rangle$, then we use a Hamiltonian operator $\hat{H}$, whether it be hermitian or non-hermitian. We know that the

Hamiltonian operator gives us an eigenvalue H when it acts on a quantum state $|\mathbf{\Psi}(\mathbf{r},t)\rangle$ as depicted in Eq. 5.

$$\hat{H}\,|\mathbf{\Psi}(\mathbf{r},t)\rangle = H\,|\mathbf{\Psi}(\mathbf{r},t)\rangle \tag{5}$$

Then, if we let the coherent state $|\alpha\rangle$ be acted on by the non-Hermitian annihilation operator $\hat{\alpha}$ we obtain a more mathematical definition of the coherent state:

$$\hat{\alpha}\,|\alpha\rangle = \alpha\,|\alpha\rangle \tag{6}$$

$$\alpha = |\alpha|\exp(\imath\phi) \tag{7}$$

Eq. 6 tells us that the coherent state $|\alpha\rangle$ is an eigenvector of the non-Hermitian annihilation operator $\hat{\alpha}$. The corresponding eigenvalue α shown in Eq. 7 is imaginary since $\hat{\alpha}$ is non-Hermitian. The imaginary part of our eigenvalue allows us to make measurements on the phase shift in the MZI while it's intensity amplitude is given by α [2]. Further mathematics of these field operators are too complex for the scope of this thesis so will be left out. The results that are obtained with the mathematics will help improve phase measurements by many orders of magnitude.

Now that we have a method for describing our coherent state in a quantum mechanical way, what we need is to figure out how the interferometer changes our coherent state as it travels through the interferometer. The change is caused by the phase shifter in the interferometer. Depending on the specific phase shifter present, a corresponding operator that describes how the phase shifter changes the input state can be derived. Usually the phase shift operators derived for an instrument such as a MZI are non-Hermitian as described above and will work for any given input state into the interferometer. For the case of the Mach-Zehnder interferometer, which is the interferometer I use in my research, the Hermitian phase shift operator $\hat{U}_\phi$ from Ref. [12] is:

$$\hat{U}_\phi = \exp\left(\imath\phi\hat{G}\right) \tag{8}$$

$$\hat{G} = \frac{\hat{n}_A - \hat{n}_B}{2} \tag{9}$$

where $\hat{G}$ contains the difference of number operators $\hat{n}_A$ and $\hat{n}_B$.

$\hat{n}_A$ is the number operator for port A and $\hat{n}_B$ is the number operator for port B. These number operators perform the task of creating and annihilating the photons which is how a state is changed in the MZI [11]. The port A number operator $\hat{n}_A = \hat{a}^\dagger a$ where $\hat{a}^\dagger$ is the creation operator and a is the annihilation operator. Similarly for port B's number operator.

When our coherent state $|\alpha\rangle$ is acted upon by the phase shift operator $\hat{U}_\phi$ one obtains:

$$\hat{U}_\phi\,|\alpha\rangle = \exp\left(\imath\phi\right)|\alpha\rangle \tag{10}$$

Since a coherent state is the sum of all possible photon numbers we obtain the same eigenstate that we started with as Eq. 10 shows. Also, the eigenvalue that the phase shift operator

$\hat{U}_\phi$ produces is imaginary due to our phase shift operator $\hat{U}_\phi$ being non-Hermitian. Most importantly though is that the eigenvalue is not dependent on the number of photons in our system. It is as though we are counting photons one at a time. This gives us a method for determining the phase estimation limit of coherent light based interferometry.

3.A.1. Coherent State Sensitivity

Heisenberg's uncertainty principle in terms of energy and time $\Delta E \Delta t \geq \hbar$ can provide us with the phase estimation limit that we seek. Since we are considering individual photons, quantum electrodynamics gives us the energy of these individual photons in terms of the angular frequency ω as shown in Eq. 11. The phase shift ϕ can be given in terms of the angular frequency ω by Eq. 12.

$$E_\gamma = \hbar n \omega \tag{11}$$

$$\phi = \omega t \tag{12}$$

$\hbar$ is Plank's constant, n is the mean number of photons in the MZI at any given time, and ω is the angular frequency of the photon. If we assume that the uncertainty in the values of energy and time are small then we can approximate their respective uncertainties as $\Delta E_\gamma = \hbar n \Delta\omega$ and $\Delta\phi = \omega \Delta t$. After solving this latter equation for Δt, we can insert E_γ and Δt into Heisenberg's uncertainty principle given above. We obtain a new uncertainty principle in terms of the phase shift specifically for our coherent light based MZI [2]. This is given as:

$$\Delta n \Delta\phi \geq 1 \tag{13}$$

$$\Delta\phi_{SNL} = \frac{1}{\sqrt{n}} \tag{14}$$

The mean photon number fluctuation is given by $\Delta n = \sqrt{n}$. After plugging this result into Eq. 13 we obtain what is called the shot-noise limit (SNL) for coherent light based interferometry as presented in Eq. 14. After solving $\Delta\phi_{SNL}$ for Δx_{SNL} it is found that the sensitivity for measuring path length difference Δx is now proportional to the wavelength of light λ divided by the square root of the mean number of photons n. For LIGO the value of λ is about $1\mu m$ and n is about 10^{24} photons since LIGO uses a circulating power of about 100kW. After doing an order of magnitude calculation, our new $\Delta x \approx 10^{-18}$m. This is the precise value where theory predicts to begin seeing gravitational waves. Thus, by using a quantum description of light, called the coherent state, we improve LIGO's sensitivity by twelve orders of magnitude from the classically calculated sensitivity limit.

3.B. Squeezed States

A squeezed state of light was first proposed in 1981 by Carlton Caves [13]. The idea of a squeezed state in terms of the fluctuations $\Delta\phi$ and Δn in the MZI is that you can decrease

the uncertainty in one fluctuation at the expense of the other while still satisfying the uncertainty principle of Eq. 13 [13]. In other words, we can work around Heisenberg's uncertainty principle. The idea is that we can improve accuracy in one dimension by reducing accuracy in the other. Which one you choose depends on which measurement you are more interested in. In our study of improving phase estimation we would like to squeeze $\Delta\phi$ and elongate Δn. One way to achieve a squeezed state of light is by inputting an entangled state of light into the MZI [2].

In the two schemes that we have considered so far we have had no quantum entanglement. Quantum states may become entangled when two or more quantum particles such as a photon interact and share information such as spin, momentum, or polarization [14]. If we have two states, say $|\psi_\alpha\rangle$ and $|\psi_\beta\rangle$, that are entangled, then by taking a measurement of one we automatically know the outcome of the other. This property, only allowed in the laws of quantum mechanics, provides us with a new tool that we can use in our MZI to improve measurement sensitivity.

We can take advantage of this property by considering port B in the MZI as shown in Fig. 1b. So far we have not considered any input into port B. Another way to describe putting nothing into port B is to say that you are inputting a vacuum state $|0\rangle$ into it. Instead of putting a vacuum state into port B we can input a state that is entangled with the state in port A. In interferometric terms we call this 'two-mode.' Now that we have a means to make measurements of the phase shift ϕ, and therefore the path length difference x, by using entanglement in a MZI, we must decide on what squeezed entangled states to use.

There are many proposed entangled quantum states of light that can be used in a MZI such as the two-mode squeezed vacuum (TMSV) state [12] and the NOON state [15]. In the following section I will consider the NOON state because it is a relatively simple state and because the Quantum Sciences and Technologies (QST) group at LSU that I work with has a significant amount of research that uses the NOON state.

3.C. NOON State

The NOON state is given by [2]:

$$|NOON\rangle = |N\rangle_A |0\rangle_B + |0\rangle_A |N\rangle_B \tag{15}$$

and first appeared in the context of quantum interferometry as a footnote in a paper by our group on quantum interferometry [8]. The term 'high-NOON' state is often used instead of just NOON state indicating that the total photon number N is large [2]. This total photon number represents the total number of photons that you are counting when you make a measurement. In current experimental setups N is normally small, about 3 or 4, because it is rather difficult to entangle many photons simultaniously using today's technology. In theory,

the number of entangled photons could approach infinity with the appropriate technology. In the case of the NOON state $|NOON\rangle$ we measure that either all of the photons came from port A and vacuum came from port B or all of the photons came from port B and vacuum came from port A. This idea of only one state or the other occurring puts the NOON state in a class of entangled states coined Schrödinger cat states.

The phase shift operator $\hat{U}_\phi$ of Eq. 8 will work in describing how the phase shifter changes our NOON state coming in from ports A and B. Since I have either all of the photons coming into port A or port B, Eq. 9 simplifies to just one photon number operator instead of two. After letting $\hat{U}_\phi$ act on $|NOON\rangle$ we obtain Eq. 16, which is similar to Eq. 10

$$\hat{U}_\phi |\alpha\rangle = \exp(\imath N\phi) |\alpha\rangle \tag{16}$$

As with the coherent state, we obtain the same eigenstate that we started with and the eigenvalue is again imaginary. The difference between the coherent state and the NOON state is that the latter is dependent on the number of photons N that we measure. This peculiarity of the entangled NOON state allows for phase sensitivity that beats the SNL. Beating the SNL is termed 'super-sensitivity' [2].

3.D. NOON State 'Super-Sensitivity'

The measurable that gives us a detection signal M at the output of a MZI for our coherent state and NOON state comes from the eigenvalues of Eq. 10 and Eq. 16. By plotting these signals versus the phase shift ϕ in Fig. 4 we can compare their sensitivities.

By using the same strategy that led us to Eq. 4, we can find the phase sensitivity of a NOON state denoted as $\Delta\phi_{NOON}$. What we find is the following:

$$\Delta\phi_{NOON} = \frac{1}{N} \tag{17}$$

The $1/N$ scaling of the $\Delta\phi_{NOON}$ increases our sensitivity much faster than the $1/\sqrt{N}$ scaling of $\Delta\phi_{SN}$ giving us better than shot-noise limited sensitivity. The scaling of phase sensitivity with a NOON state is equal to the scaling that Heisenberg's uncertainty principle imposes upon phase estimation which is also $1/N$. Thus, an entangled state such as a NOON state can obtain 'super-sensitivity' [2].

4. Two-Mode Squeezed Vacuum State

Previously, I showed that quantum states such as a coherent state and a NOON state can improve upon phase sensitivity of classical interferometry by many orders of magnitude. In the case of the Michelson interferometer at LIGO a coherent state improves the sensitivity by about twelve orders of magnitude, while the entangled NOON state can do much better still [2]. In reality it is difficult to reach 'ultra-sensitivity' using these NOON states in a

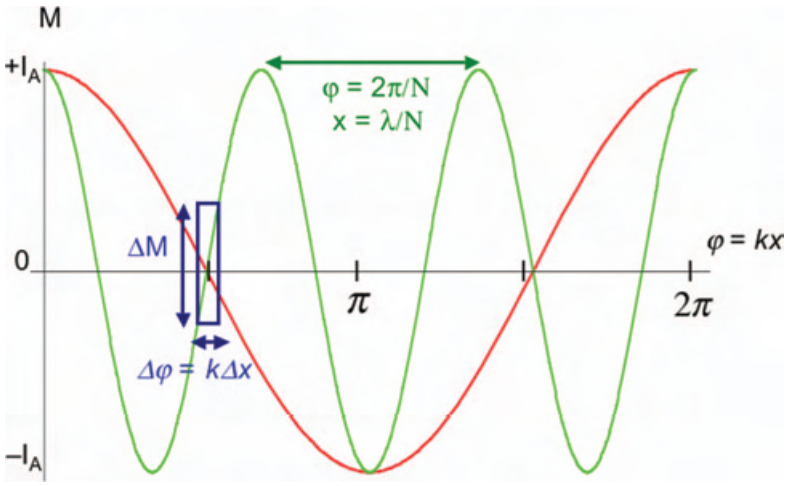

Fig. 4: A comparison of detection signals between the coherent state (red) and the NOON state (green) [2]. Since the NOON state oscillates N times as fast we see that the slope of the graph is much steeper which allows for much more accurate phase estimations.

MZI because we would need to entangle many photons, which is a difficult task with today's technology. Other entangled states may be used to reach 'ultra-sensitivity' that is easier to implement experimentally. This is where my research comes in.

Significant advances have been made in quantum enhancement of phase sensitivity [18] and the meaning of Heisenberg limit has been thoroughly examined [19]. Yet, a recently proposed phase estimation scheme dips below the HL in the case of infinite number of parity measurements [12]. This scheme is based on measuring the parity of the state of light at the output of a Mach-Zehnder interferometer (MZI), Fig. 5a, with two-mode squeezed vacuum (TMSV) input. It turned out that this particular scheme using TMSV input has sub-Heisenberg sensitivity even with linear phase evolution. This is due to the fact that the photon number uncertainty for the state of light inside of MZI is greater than an average photon number used for the measurement [20, 21].

In my research I consider an entangled state that is called two-mode squeezed vacuum (TMSV). This TMSV state $|TMSV\rangle$ is a superposition of twin Fock states where the term Fock state is just another way to say number state. Unlike the NOON state, the TMSV state considers a given number of entangled photons in both mode A and B at the same time. This means that the TMSV state is not in the class of Schrödinger class states. For the TMSV state inputted into the MZI I used a small number of entangled photons that may be attained experimentally with today's technology. Using photon number counting statistics made on the measurement at the output of a MZI using the TMSV state and a low number

of entangled photons, my work shows that 'super sensitivity' can be obtained in a finite number of measurements.

The advantage of our proposed phase estimation scheme is its experimental feasibility. Squeezed vacuum generation in an optical parametric amplifier (OPA) of up to 12 dB of quadrature squeezing has been achieved experimentally [22]. This, in turn, translates to a mean photon number in both modes of the TMSV of up to seven photons. Hence, the parity, even or odd photon number, of the state can be measured with existing photon-number-resolving detectors such as transition edge sensors [23, 24]. However, a photon-number-resolving detector does not provide a mean value of the parity signal after a single measurement, which means that a phase measuring experiment must be repeated multiple times.

Assuming a flat a priori distribution, our paper applies Bayesian analysis to the TMSV based phase-estimation scheme where photon-number-resolving detectors are used to infer the parity signal. We use the parity signal at the output of the MZI to estimate the unknown phase θ. Our analysis shows that, although phase estimation is biased near the phase origin and at $\pi/2$, there is an in-between interval where unbiased phase estimation is possible. In this interval, phase sensitivity saturates the Cramer-Rao bound (CRB) and remains below the SN limit. Unlike the aforementioned phase estimation scheme, we achieve these results with a finite number of parity measurements.

5. Model

We consider here a phase estimation scheme with input in a two-mode squeezed vacuum state (TMSV) that is commonly generated in unseeded optical parametric amplifiers. TMSV state is ideally a superposition of twin Fock states $|\psi_{\bar{n}}\rangle = \sum_{n=0}^{\infty} \sqrt{p_n(\bar{n})}\,|n,n\rangle$, where the probability p_n depends on average number of photons in both modes of TMSV, $\bar{n}$, in the following way $p_n(\bar{n}) = (1-t_{\bar{n}})t_{\bar{n}}^n$ with $t_{\bar{n}} = 1/(1+2/\bar{n})$ [25]. Propagation of the light through a MZI with linear phase accumulation imprints phase information on the state that is retrieved by measuring parity at the output of the MZI.

Parity based phase estimation was originally introduced to quantum optics by Gerry in Ref. [26] and is based on the parity of photon number detected in the state at the output of MZI. The expected value of the parity signal $\langle\hat{\Pi}\rangle$ for TMSV based phase estimation scheme,

$$\langle\hat{\Pi}\rangle = \frac{1}{\sqrt{1+\bar{n}(\bar{n}+2)\sin^2\theta}}, \tag{18}$$

was obtained in Ref. [12]. It depends on the unknown phase θ inside of the MZI and the mean photon number $\bar{n}$ in the TMSV state used. Thus, knowing $\bar{n}$ at the input and $\langle\hat{\Pi}\rangle$ at the output, the unknown phase θ can be estimated.

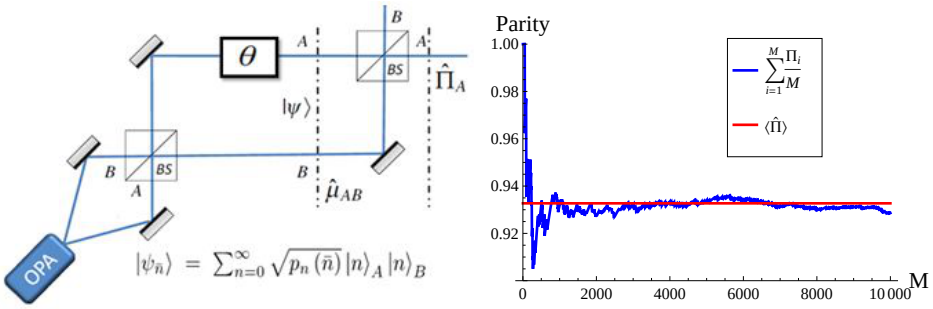

(a) Mach-Zehnder interferometer (MZI) (b) Convergence of Parity Signal

Fig. 5: (a) Two-mode squeezed vacuum states are generated at the input of the MZI by an optical parametric amplifier. We measure the parity signal at the output of the MZI with a photon number resolving detector. (b) Convergence of the parity signal based on outcomes of numerically generated detection events (blue) to the expected value of $\langle\hat{\Pi}\rangle = 0.93$ (red) in a finite number of $M = 10^4$ parity measurements. A different sample of this convergence will evolve differently due to the probabilistic nature of the scheme, but it will always converge to its expectation value. Here, we assumed that the photon number is $\bar{n} = 3$ and the unknown phase had value $\theta = 0.1$.

Each parity measurement returns either an even or odd outcome with probabilities $P_{\rm e}$ and $P_{\rm o}$. Thus, there is uncertainty in measuring the parity signal for our phase estimation scheme $\langle(\Delta\hat{\Pi})^2\rangle = 1 - \langle\hat{\Pi}\rangle^2$, where the following property $\hat{\Pi}^2 = 1$ has been used. Yet, in the limit of infinite measurement, the single shot phase sensitivity converges to $(\Delta\theta)^2 = \langle(\Delta\hat{\Pi})^2\rangle/(\frac{d\langle\hat{\Pi}\rangle}{d\theta})^2$ and implies that the uncertainty of phase estimation at the vicinity of $\theta = 0$ is $(\Delta\theta)^2 = 1/(\bar{n}^2 + \bar{n})$ that is below the HL.

In practice, the parity measurement can be implemented with photon-number resolving detectors. Using 100% efficient photon-number-resolving detectors at an output of MZI with TMSV input, one expects to detect n photons with probability $P(n) = \sum_{m>n/2}^{\infty} p_m(\bar{n})[d^m_{n-m,0}(\theta+\pi/2)]^2$, where $p_m(\bar{n})$ is probability of having $|m,m\rangle$ state and $d^m_{\mu,\nu}(\theta)$ is a rotation matrix element. Inferring parity of the state disregards an actual number of photons detected and focuses on whether this number is even or odd. The probability of detecting an even photon number is then $P_{\rm e} = \sum_{i=0}^{\infty} P(2i)$, where summation can be easily evaluated to

$$P_{\rm e} = \frac{1}{2}\left(1 + \langle\hat{\Pi}\rangle\right) \tag{19}$$

since $P_e + P_o = 1$ and the expectation value of a state's parity is $\langle\hat{\Pi}\rangle = 1 \cdot P_e + (-1) \cdot P_o$.

Fig. 5b shows how an inferred parity signal (blue) converges to its expected value of

$\langle\hat{\Pi}\rangle = 0.93$ (red) in a set of $M = 10^4$ parity measurements. Here, we use the probability of an even photon number, P_e from Eq. (19), in order to numerically generate a possible parity measurement record with an averaged input photon number $\bar{n} = 3$ and an unknown phase $\theta = 0.1$. Due to the probabilistic nature of the scheme, repetition of this procedure with the same parameters would obviously result in a slightly different measurement record. Hence, in any experiment there will always be an uncertainty in the inferred parity signal that leads to an uncertainty in the estimation of the unknown phase θ.

The statistics of the inferred variable ϕ is fully determined by the statistics of the measured events P_e. A Bayesian approach to interferometry provides an interval estimation and may be regarded as a distribution of probability in the sense of degrees of belief [27]. So we analyze a parity measurement record at the output of the MZI using Bayes' theorem and obtain a probability for the unknown phase θ to be in the interval $[\phi, \phi+d\phi]$ given all prior observations and a flat prior distribution. After each measurement, the probability density function (PDF) is updated according to the Bayes' theorem: $P(\phi|\text{output}) \propto \text{P}(\text{output}|\phi)\text{P}_{\text{prior}}(\phi)$, so that each consecutive observation modifies the PDF and improves phase estimation. Hence, the update equation given by Bayes' theorem for an even or odd outcome is:

$$P(\phi|\{e,o\}) \propto P(\{e,o\}|\phi)P(\phi). \tag{20}$$

Particular outcomes in our numerical model are independent thus the Bayesian PDF after M runs with m even outcomes is:

$$P(\phi|m) \propto P_e^m(\phi)P_o^{M-m}(\phi), \tag{21}$$

that provides estimation interval with PDF's maximum corresponding most probable phase estimation.

Fig. 6 presents use of this update rule in the case of $M = 200$ runs with $\bar{n} = 3$ input photons for different number of even outcomes: $m = 150,\ 175,\ 200$. The heights of each have been rescaled for the ease of comparison. One can see two effects that reduced number of even outcomes has on the PDF. The PDF becomes broader and shifts its maximum towards $\phi = \pi/2$. This results in higher phase uncertainty and thus reduction in the sensitivity of phase estimation if unknown phase is near $\theta = \pi/2$. This coincides with predictions of Ref. [12] that the best phase sensitivity is achieved in the vicinity of $\theta = 0$, where the parity of the output state is predominantly even.

6. Numerical results

In contrast to an assumed number of even outcomes discussed in Fig. 6, actual statistics of a finite-length measurement record is governed by the following probability of even outcomes:

$$P_e = \frac{1}{2}\left(1 + \frac{1}{\sqrt{1+\bar{n}(\bar{n}+2)\sin^2\theta}}\right), \tag{22}$$

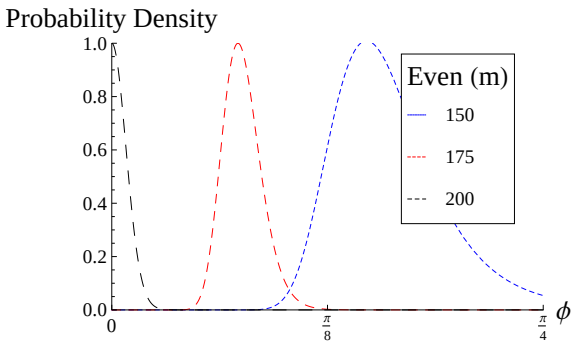

Fig. 6: The Bayesian probability density function (PDF) from Eq. (21) is evaluated with mean photon number $\bar{n} = 3$ and $M = 200$ parity measurements for various number of even outcomes m. We rescaled the heights for easier comparison of their widths and maxima. As the number of even outcomes decreases from $m = M$ to $m = 0.75M$, the maximum of the PDF shifts towards $\phi = \pi/2$ with a consequent broadening of the distribution that reduces the accuracy of phase estimation in this region.

that comes directly from Eq. (19) and allows to model phase estimation with TMSV and parity detection numerically. Choosing the input photon number $\bar{n}$ and an unknown phase θ makes the probability of even outcomes P_e become a number that we use to numerically generate a measurement record of finite length M. From such a record, we determine a number of even outcomes m and obtain Bayesian PDF using update rule from Eq. (21). We base our single phase estimation on locating the phase, ϕ, at the maximum of Bayesian PDF.

There are four local maxima of Bayesian PDF on a 2π interval due to the periodicity of the parity signal and its invariance under inversion $\theta \to -\theta$. Hence, unique phase values belong to the interval $\theta \in (0, \pi/2]$ where Bayesian PDF has a single maximum and will be used for local phase estimation. In addition to the phase estimation, Bayesian PDF provides an estimation interval that can be associated with the width of a Bayesian PDF. In our case however, we adopt a different approach to the calculation of such an interval so that we better reflect effects of the measurement record length.

The most prominent effect of the record length on the phase estimation is the lack of reproducibility due to finite deviation from expected value of the parity signal. As an example, we have considered the family of $N = 10^3$ parity measurement records generated for $\theta = 0.08$ and $\bar{n} = 3$ and $M = 200$ long. Fig. 7 shows the distribution of phase estimations, $\phi \in [0, \pi/2]$, for a measurement record in the family. There are three noteworthy points. First, possible phase estimations are discrete and sparse near $\phi = 0$, which is associated with a number of odd outcomes in the measurement record. Second, the distribution has a mean

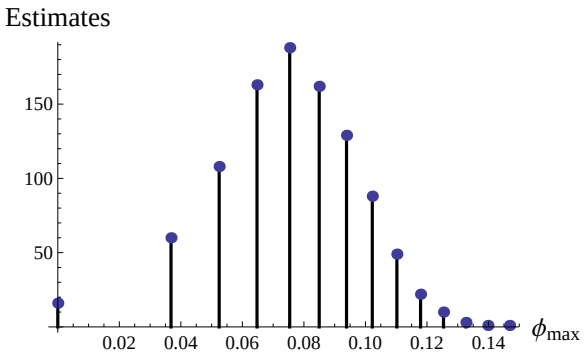

Fig. 7: Distribution of obtained phase estimations in a family of $N = 10^3$ measurement records numerically generated for $\theta = 0.08$ and $\bar{n} = 3$. It shows uncertainty of phase estimation, ϕ, due to a finite length of parity measurement record $M = 200$. This distribution has the mean value of $\bar{\phi} = 0.078$ and a standard deviation of $\Delta\bar{\phi} = 0.022$ that characterizes uncertainty of phase estimation after finite number of measurements.

value of $\bar{\phi} = 0.078$; hence, on average one would get a phase estimation with some bias, defined as $\mathrm{B} = \bar{\phi} - \theta$. The final point, however, is that there is a spread of possible phase estimations with a standard deviation of $\Delta\bar{\phi} = 0.022$; hence, we will associate sensitivity of the phase estimation with this standard deviation.

7. Bias in phase estimation

As we ran our phase estimator with input intensity $\bar{n} = 3$ for several unknown phases, $\theta \in [0, \pi/2]$, we found the presence of bias, which is statistical favouritism that causes misleading results, defined as $Bias = \bar{\phi} - \theta$.

Fig. 8 demonstrates high bias in estimating the unknown phase near the boundaries of the interval. This is shown for different lengths of measurement records M. It demonstrates that longer measurement records do not suffer from bias. Yet, for an unknown phase $\theta \in [0, 0.08]$, our phase estimation exhibits a large bias toward zero. Likewise, when the unknown phase approaches $\pi/2$ our scheme again becomes biased. This leaves an optimal phase interval of $\theta \in [0.08, 0.6]$ that offers unbiased phase estimation.

The interval for unbiased phase estimation depends on the input intensity $\bar{n}$. For a larger $\bar{n} = 7$, our phase estimator shows that the minimum value of the unbiased phase interval remains relatively unchanged; however, the length of the interval reduces due to signal localization near the phase origin. Namely, the right boundary of the interval reduces from $\theta = 0.6$ to $\theta = 0.3$.

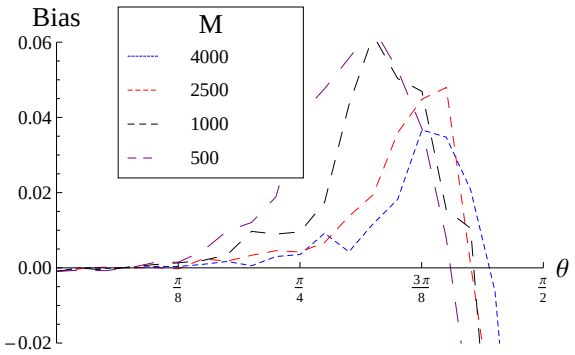

Fig. 8: Bias of phase estimation for TMSV with $\bar{n} = 3$ photons as a function of the unknown phase θ. For a $N = 10^3$ family of measurement records, we are increasing the length of the parity measurement records M. Bias is negligible in the interval $\theta \in [0.08, 0.6]$, and thus provides us with an accurate phase estimation scheme.

8. Phase sensitivity

The uncertainty of phase estimation $\Delta\phi$ quantifies the phase sensitivity of the scheme. In the case of conventional phase estimation with coherent laser light and intensity difference measurement, phase sensitivity is shot-noise limited, $\Delta\phi > 1/\sqrt{M\bar{n}}$. This sensitivity improves with increasing input intensity as well as the length of the measurement record. However, ultimate phase sensitivity is HL, $\Delta\phi > 1/\sqrt{M\bar{n}^2}$, that has the same dependence on the length of measurement record M but faster dependence on input photon number.

In the limit of large number of parity measurements, phase estimation with TMSV and parity detection is capable of beating the HL due to a greater photon number variance in the state. Phase sensitivity for this scheme is equal to [12]:

$$\Delta\phi = \frac{1 + \bar{n}(2+\bar{n})\sin^2\theta}{\sqrt{M\bar{n}(2+\bar{n})}\cos\theta}. \tag{23}$$

Hence, an optimum phase sensitivity, $\Delta\phi = 1/\sqrt{M\bar{n}(2+\bar{n})}$, obtained near $\theta = 0$ is sub-Heisenberg.

In the case of finite-length measurement records, measuring parity with photon-number-resolving detectors is however biased near $\theta = 0$. Thus, Bayesian phase estimation with photon-number resolving detectors can only be obtained in the low bias interval of $\theta \in [0.08, 0.6]$. Fig. 9 shows the standard deviation, $\Delta\bar{\phi}$, of our phase estimation scheme. Increasing the number of runs in a phase estimate improves the phase sensitivity when θ is near the origin. This is because phase uncertainty scales as $\Delta\phi = c/\sqrt{M}$, where the proportionality constant c depends on the unknown phase θ and input photon number $\bar{n}$. As

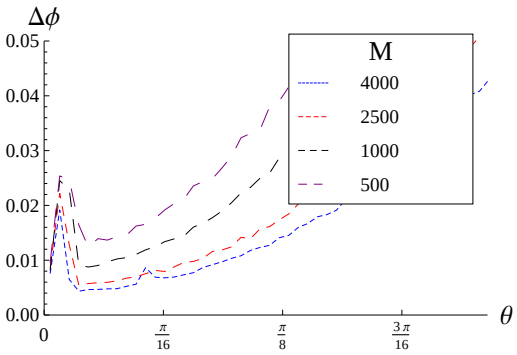

Fig. 9: The standard deviation of phase estimation with an input photon number of $\bar{n} = 3$ for increasing number of numerical runs M. We found that more phase estimates reduces the standard deviation. As θ increases towards $\pi/2$ the standard deviation becomes large. This explains why bias is high when $\theta > 0.6$.

we calculate the unknown phase θ in various regions of bias with $\bar{n} = 3$, we find that the standard deviation is low near the origin.

As an example, consider $\theta = 0.01$ which is in a region of high bias. As we increase the number of numerical runs in a phase estimate, we find that the standard deviation remains constant and cannot be fitted to a $c/\sqrt{M}$ function in order to determine the proportionality coefficient c (see Fig. 10). The same behavior is observed in the other high-bias interval closer to $\pi/2$.

In the following, we focus on unknown phases in the interval suitable for unbiased phase estimation with parity measurement using photon number resolving detectors. Our data does have the expected $1/\sqrt{M}$ dependence. Hence, we can compare the proportionality coefficient obtained from the fitting procedure with a value expected from the CRB as well as from the SN limit.

Fig. 11 presents the standard deviation of phase estimation as a function of the number of phase estimates for an unknown phase of $\theta = 0.3$ and $\bar{n} = 3$. In this case, we find that the proportionality coefficient is $c_{\mathrm{TMSV}} = 0.69$. As we compare this proportionality coefficient with the SN limit, $c_{\mathrm{SN}} = 0.58$, and the CRB, $c_{\mathrm{CRB}} = 0.62$, obtained from Eq. (23), we see that the sensitivity is in close proximity to the CRB (red). With an unknown phase of $\theta = 0.08$ located closer to the phase origin in our unbiased interval we can improve this result. For a given unknown phase, the sensitivity of phase estimation could be improved by varying the mean photon number in the input TMSV state. This is analysed for $\theta = 0.3$ and the results are presented in Fig. 12, where the phase sensitivity is characterized by c_{TMSV} which removes the dependence on M and focuses on input intensity dependence. One

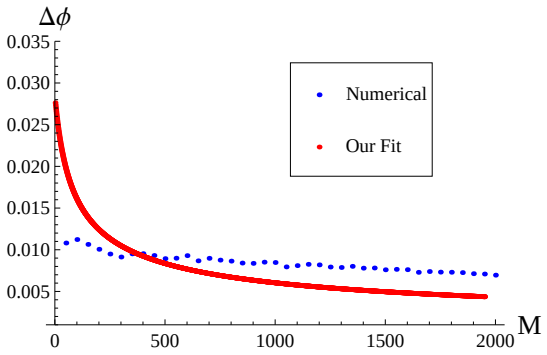

Fig. 10: For a single phase estimate we see how the standard deviation changes for increasing numberical runs M with $\bar{n} = 3$ and unknown phase $\theta = 0.01$. We compare our results with that of the Cramer-Rao bound (CRB) and shot-noise (SN) limits. Since $\theta = 0.01$ is in a high biased region, the data does not have the $1/\sqrt{M}$ dependence. We can obtain this dependence with the use of an unknown phase in the unbiased region as shown in Fig. 11.

can see that our previous choice of $\bar{n} = 3$ is an optimum input intensity for this value of the unknown phase. For lower input intensities, phase sensitivity is in close proximity to the CRB. As the input intensity increases, the standard deviation of the current scheme becomes much worse than predicted by the CRB. Therefore, we investigate lower unknown phases in our unbiased interval. The best sensitivity of our phase estimation protocol is expected near the phase origin. Performing phase estimation in the unbiased interval offers significant improvement for phase sensitivity. With an unknown phase of $\theta = 0.08$ shown in Fig. 13, one can see that phase sensitivity of our scheme is nearly optimal and beats the SN limit for an extended range of input intensities. Thus, parity measurement with photon-number-resolving detectors is close to the limiting performance for our scheme and could be used to demonstrate sub-Heisenberg limited phase estimation.

9. Conclusion

Phase estimation protocols that rely on parity measurement benefit from photon number-resolving-detectors that can be used to infer parity of the state. Here, we considered a particular phase estimation protocol that is based on TMSV input and parity detection at the output of the MZI. Use of photon-number-resolving detectors means that measurements must be repeated multiple times with Bayesian analysis applied to all outcomes.

Our scheme shows that phase sensitivity saturates the Cramer-Rao bound and beats the Heisenberg limit with the use of a finite number of experimental runs. We discovered that our maximum likelihood estimator is biased near the phase origin where the best sensitivity

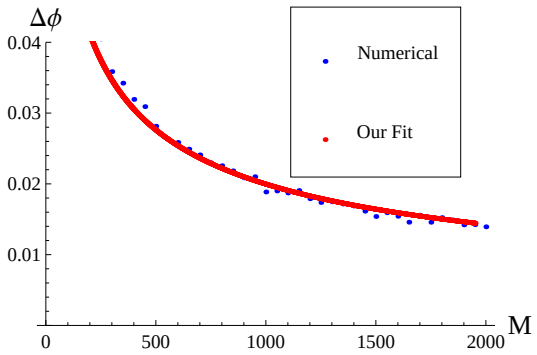

Fig. 11: The standard deviation versus the number of numerical runs M in the case of unknown phase $\theta = 0.3$ and photon number $\bar{n} = 3$. It exhibits the expected $1/\sqrt{M}$ scaling with a proportionality coefficient, $c_{\mathrm{TMSV}} = 0.69$. It does not beat either $c_{\mathrm{CRB}} = 0.62$ or $c_{\mathrm{SN}} = 1/\sqrt{\bar{n}} = 0.58$, but we can use an unknown phase of $\theta = 0.08$ which is at the lower end of our unbiased interval to significantly improve this result.

is expected. As a result, the standard deviation of the estimated values does not reduce with increasing number of phase estimations but stays constant. However, small values of the unknown phase in our unbiased interval $\theta \in [0.08, 0.6]$ allow for unbiased phase estimation. Phase sensitivity behaves as expected and remains in close proximity to the Cramer-Rao bound. Consequently, the phase sensitivity remains sub-shot-noise limited for a broad range of input intensities as long as phase estimation is performed near the origin.

Acknowledgments

We would like to acknowledge the Intelligence Advanced Research Projects Activity and the National Science Foundation for financial support. I thank Petr Anisimov for all of his help and guidance throughout the course of this research. I thank Dr. Jonathan Dowling for being a great mentor throughout my undergraduate experience. Also, I would like to thank my thesis defense committee: Dr. Jonathan Dowling from the Department of Physics and Astronomy at LSU, Dr. Hwang Lee from the Department of Physics and Astronomy at LSU, and Dr. Jimmie Lawson from LSU's department of Mathematics.

References

1. A. A. Michelson and E. W. Morley, "On the Relative Motion of the Earth and the Luminiferous Ether," American Journal of Science **34**, 333–345 (1887).
2. J. P. Dowling, "Quantum optical metrology the lowdown on high-n00n states," Contemp. Phys. **49**, 125–143 (2008).

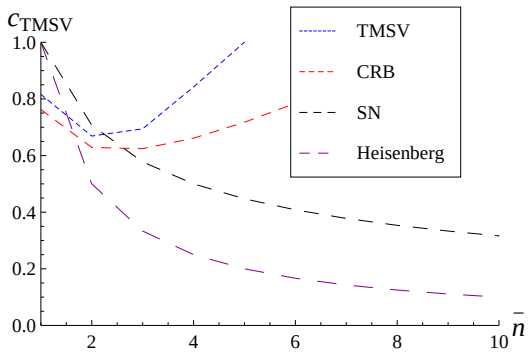

Fig. 12: The constant of proportionality, c_{TMSV}, versus the number of photons in the input state for an unknown phase of $\theta = 0.3$. The case of $\bar{n} = 3$ has the smallest standard deviation for phase estimation based on the scheme presented here (blue). The demonstrated sensitivity is in close proximity to the CRB in red. The SN limit in black and the Heisenberg limit (HL) in purple are present for comparison.

3. L. Mandel and E. Wolf, *Optical Coherence and Quantum Optics* (Cambridge University Press, 1995), 1st ed.
4. H. J. Kimble, M. Dagenais, and L. Mandel, "Photon Antibunching in Resonance Fluorescence," Physical Review Letters **39**, 691–695 (1977).
5. G. Watson and J. R. Klauder, "Generalized affine coherent states: A natural framework for quantization of metric-like variables," J.MATH.PHYS. **41**, 8072 (2000).
6. C. W. Gardiner and P. Zoller, *Quantum Noise: A Handbook of Markovian and Non-Markovian Quantum Stochastic Methods with Applications to Quantum Optics (Springer Series in Synergetics)* (Springer, 2004), 3rd ed.
7. G. Breitenbach, S. Schiller, and J. Mlynek, "Measurement of the quantum states of squeezed light," Nature **387**, 471–475 (1997).
8. H. Lee, P. Kok, and J. P. Dowling, "A quantum rosetta stone for interferometry," J. Mod. Opt. **49**, 2325–2338 (2002).
9. E. C. G. Sudarshan, "Equivalence of Semiclassical and Quantum Mechanical Descriptions of Statistical Light Beams," Physical Review Letters **10**, 277–279 (1963).
10. E. Schrdinger, "Der stetige bergang von der mikro- zur makromechanik," Die Naturwissenschaften **14**, 664–666 (1926).
11. R. P. Feynman, *Statistical Mechanics: A Set Of Lectures (Advanced Books Classics)* (Westview Press, 1998), 2nd ed.
12. P. M. Anisimov, G. M. Raterman, A. Chiruvelli, W. N. Plick, S. D. Huver, H. Lee, and

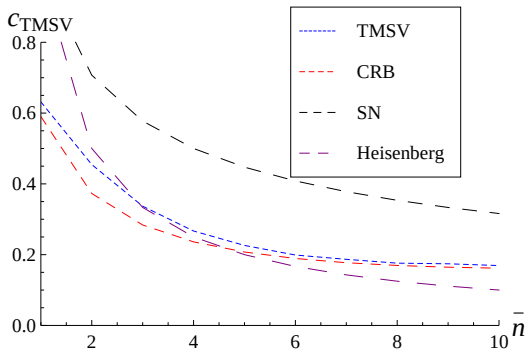

Fig. 13: The constant of proportionality, c_{TMSV}, versus the number of photons in the input state for an unknown phase of $\theta = 0.08$. Our numerical experiment (blue) does much better than SN (Black), almost as well as the CRB (red), and does as well as the HL (purple).

J. P. Dowling, "Quantum metrology with two-mode squeezed vacuum: Parity detection beats the heisenberg limit," Phys. Rev. Lett. **104**, 103602 (2010).

13. C. M. Caves, "Quantum-Mechanical Radiation-Pressure Fluctuations in an Interferometer," Physical Review Letters **45**, 75–79 (1980).
14. M. Tegmark and J. A. Wheeler, "100 Years of the Quantum," (2001).
15. B. C. Sanders, "Quantum dynamics of the nonlinear rotator and the effects of continual spin measurement," Phys. Rev. A **40**, 2417–2427 (1989).
16. C. C. Gerry and J. Mimih, "The parity operator in quantum optical metrology," Contemp. Phys. **51**, 497–511 (2010).
17. R. A. Campos, C. C. Gerry, and A. Benmoussa, "Optical interferometry at the heisenberg limit with twin fock states and parity measurements," Phys. Rev. A **68**, 023810 (2003).
18. V. Giovannetti, S. Lloyd, and L. Maccone, "Advances in quantum metrology," Nature Photonics **5**, 222–229 (2011).
19. M. Zwierz, C. A. Prez-Delgado, and P. Kok, "Ultimate limits to quantum metrology and the meaning of the heisenberg limit," .
20. H. F. Hofmann, "All path-symmetric pure states achieve their maximal phase sensitivity in conventional two-path interferometry," Phys. Rev. A **79**, 033822 (2009).
21. P. Hyllus, L. Pezzé, and A. Smerzi, "Entanglement and sensitivity in precision measurements with states of a fluctuating number of particles," Phys. Rev. Lett. **105**, 120501 (2010).
22. M. Mehmet, H. Vahlbruch, N. Lastzka, K. Danzmann, and R. Schnabel, "Observation of squeezed states with strong photon-number oscillations," Phys. Rev. A **81**, 013814

(2010).

23. B. Cabrera, R. Clarke, P. Colling, A. Miller, S. Nam, and R. Romani, "Detection of single infrared, optical, and ultraviolet photons using superconducting transition edge sensors," App. Phys. Lett. **73**, 735–737 (1998).
24. K. Irwin and G. Hilton, "Transition-edge sensors," in "Cryogenic Particle Detection," , vol. 99 of *Topics in Applied Physics*, C. Enss, ed. (Springer Berlin / Heidelberg, 2005), pp. 81–97.
25. C. Gerry and P. Knight, *Introductory quantum optics* (Cambridge University Press, 2005).
26. C. C. Gerry, "Heisenberg-limit interferometry with four-wave mixers operating in a nonlinear regime," Phys. Rev. A **61**, 043811 (2000).
27. M. Zawisky, Y. Hasegawa, H. Rauch, Z. Hradil, R. Myska, and J. Perina, "Phase estimation in interferometry," Journal of Physics A: Mathematical and General **31**, 551 (1998).